

# Vertical Structure of Accretion Discs with Hot Coronae in AGN

A. Róžańska<sup>1</sup>, B. Czerny<sup>1</sup>, P.T. Życki<sup>1,2</sup>, G. Pojmański<sup>3</sup>

<sup>1</sup> *Nicolaus Copernicus Astronomical Center, Bartycka 18, 00-716 Warsaw, Poland*

<sup>2</sup> *Department of Physics, University of Durham, South Road, Durham DH1 3LE, England*

<sup>3</sup> *Astronomical Observatory of Warsaw University, Aleje Ujazdowskie 4, 00-478 Warsaw, Poland*

7 August 2018

## ABSTRACT

We study vertical structure of radiation pressure dominated disc with a hot corona. We include all the relevant processes like bound–free opacity and convection. We show that the presence of the corona modifies considerably the density and the opacity of the disc surface layers which are important from the point of view of spectrum formation. The surface of the disc with a corona is much denser and less ionized than the surface of a bare disc. Such a disc is likely to produce a neutral reflection and a local spectrum close to a black body. This effect will help to reconcile the predictions of accretion disc models with the observational data since a neutral reflection and a lack of Lyman edge are generally seen in AGN.

**Key words:** galaxies: active – quasars: emission lines, accretion, accretion discs – line: formation – line: profiles.

## 1 INTRODUCTION

Although it is widely believed that accretion onto supermassive black hole is the ultimate source of power in AGN we are still far from understanding the details of this process.

Recent multiwavelength observations clearly show that the gas in the vicinity of the center forms a complex multiphase medium. Cold gas is seen due to its imprints on the reflected X-ray radiation (Pounds et al. 1990) whilst hot plasma is responsible for the hard X-ray emission (for a review, see Mushotzky, Done & Pounds 1993). The cold medium is also thought to be responsible for the optical/UV/Soft X-ray emission, i.e. big bump.

The geometrical arrangement of the two phases is not clear but the most attractive model consists of an accretion disc surrounded by a hot corona, with the energy being released in both phases (e.g. Edelson et al. 1997 for NGC 4151). The disc in some objects may possibly be disrupted in its innermost part (e.g.  $\sim 10R_{Schw}$  for NGC 5548; Loska & Czerny 1997) and the flow may be dominated by advection (e.g. Narayan, Kato & Tonma 1997).

There is, however, one problem which seems to be difficult to accommodate within that scenario and which served frequently as an argument against the very existence of accretion discs in AGN. Namely, all realistic disc models predicted strong atomic features, including strong Lyman edge whilst no such feature was clearly detected in most of the AGN spectra (Antonucci 1993; see also Blaes & Agol 1996).

The problem cannot be overcome by assumption that the disc surface is highly ionized and therefore no Lyman edge is expected because the X-ray reflection puts a clear limit on the ionization parameter  $\xi$  for a number of Seyfert 1 galaxies of order of 200 (Życki et al. 1994). A huge Lyman edge is seen from the gas irradiated by X-rays with such a value of  $\xi$ , and it is still clearly seen if  $\xi$  is an order of magnitude higher (e.g. Collin-Souffrin et al. 1996). The Lyman edge disappears completely only if the temperature of the gas is above 1 million K or  $\xi$  is above 3000 which is clearly excluded by X-ray data.

In this paper we show that this apparent problem disappears if the boundary conditions between the disc and the corona are described appropriately. The basic effect is the hydrostatic pressure exerted on the disc surface by the corona which leads to much higher densities at the disc surface then adopted in typical computations which forces the local emission of the surface to be close to a black body. We also study the effect of the corona on the disc interior.

## 2 THE MODEL

### 2.1 Global disc parameters

The structure of the corona depends on the total flux,  $F_d + F_c$ , generated in the disc and in the corona, and the local Keplerian velocity,  $\Omega_K$ . Both values can be determined at a

arXiv:astro-ph/9811380v1 24 Nov 1998

given radius  $r$  from the mass of the black hole,  $M$ , and the accretion rate  $\dot{M}$  through the usual relations:

$$\Omega_K = \left( \frac{GM}{r^3} \right)^{1/2} \quad (1)$$

and

$$F_d + F_c = \frac{3GM\dot{M}}{8\pi r^3} f(r) \quad (2)$$

where  $f(r)$  represents the boundary condition at the marginally stable orbit

$$f(r) = 1 - (3R_{\text{Sch}}/r)^{1/2} \quad (3)$$

in the Newtonian approximation.

The value of the ratio  $f$  given by the formula:

$$f = \frac{F_c}{F_d + F_c} \quad (4)$$

is the free parameter in the model.

We frequently use dimensionless accretion rate,

$$\dot{m} \equiv \frac{\dot{M}}{\dot{M}_{Edd}}, \quad (5)$$

where  $\dot{M}_{Edd}$  is the critical (Eddington) accretion rate

$$\dot{M}_{Edd} = \frac{L_{Edd}}{c^2 \eta} = \frac{4\pi GMm_H}{\sigma_T c \eta}, \quad (6)$$

assuming the efficiency of accretion  $\eta = 1/12$ , as it results from the Newtonian approximation to disc accretion.

## 2.2 The vertical structure of the disc

### 2.2.1 Local viscosity model

The physics of accretion is poorly understood as the microscopic mechanism of the angular momentum transfer remains unknown. Most promising, perhaps, is the viscosity provided by the small scale magnetic field structure which develops in the disc at the expense of its rotational energy. The results of the computer simulations of this process (Balbus & Hawley 1991, 1992, Hawley, Gammie & Balbus 1995; see also Balbus & Hawley 1998 for a review) are definitely encouraging.

Therefore, as in the case of stellar convection, we restore to a replacement of all the missing physics by a single parameter  $\alpha$  introduced by Shakura & Sunyaev (1973). This kind of parameterization is very convenient. What is more, some physical attempts to describe the global effect of viscosity can be reduced to this scaling (e.g. Tout & Pringle 1992, Canuto, Goldman & Hubickyj 1984, Hawley et al. 1995).

This assumption was widely used to calculate the vertically averaged disc structure in AGN (e.g. Ross, Fabian & Mineshige 1993; see also Frank, King & Raine 1985).

It was also successfully used to calculate the vertical structure of accretion discs in cataclysmic variables leading to the discovery of the nature of dwarf novae eruptions (Meyer & Meyer-Hofmeister 1981 and Smak 1982b). The adoption of the viscosity  $\alpha$  locally allows to calculate the local behaviour of the disc. Thus the models include realistic opacities and the energy transport by convection (see Cannizzo 1994 for a recent review). There were also two-dimensional studies of models which included a complex inflow pattern (Urpin 1984, Siemiginowska 1988, Kley & Lin

1992, Różyczka, Bodenheimer & Bell 1994), consisting, for low viscosity, of outflow near equatorial plane and inflow close to the surface, but resulting in pure inflow for high viscosity ( $\alpha > 0.1$ ).

These results for cataclysmic variables cannot be easily adopted to the case of AGN accretion discs. In accretion discs in cataclysmic variables the radiation pressure is always negligible due to the presence of an extended central body.

However, certain progress has been made also in AGN discs.

The local disc structure was initially studied under an assumption that the stress is proportional to the gas pressure (not to the total pressure) (e.g. Lin & Shields 1986, Mineshige & Shields 1990). Those studies concentrated on conditions in which the ionization instability may operate. Shimura & Takahara (1993) studied the disc structure under the assumption that the energy generation rate per unit volume is proportional to the density. Outermost parts of the disc (mostly dominated by the gas pressure anyway) were studied with the  $\alpha$ -prescription e.g. by Cannizzo (1992); Cannizzo & Reiff (1992) and Huré et al. (1994a,b).

The computations of the vertical structure of the inner radiation pressure dominated parts of the disc under the assumption of the viscosity proportion to the total (i.e. gas plus radiation) pressure were postponed for a long time because of the problem of instability discovered by Pringle, Rees & Pacholczyk (1973) and discussed by Shakura & Sunyaev (1976). It was initially suggested that the disc in that region of the size of a thousand Schwarzschild radii is replaced by the hot optically thin medium (Shapiro, Lightman & Eardley 1976). However, direct observational evidences show the presence of the cold medium very close to the black hole (see Mushotzky et al. 1993 for a review and Mushotzky et al. 1995, Tanaka et al. 1995, Yaqoob et al. 1996 and a summary by Nandra et al. 1997 for the evidences of the cold disc based on the iron  $K_\alpha$  line). The theoretical reason for the disc survival is not clear although recently more advanced studies of the disc stability was undertaken (Gammie 1998). Since we do not know whether the disc survives due to the stabilizing role of the corona or the disruption of the disc leads to cold clump formation with the clumps themselves simulating the behaviour of the turbulent disc (e.g. Collin-Souffrin et al. 1996, Krolik 1998) one of the possible approaches is to explore the possible models irrespective of the potential stability problems and to verify them observationally.

Recently, the vertical structure of a radiation-pressure dominated accretion disc around a massive black hole was studied by Milson et al. (1994) and Dörrer et al. (1996). We follow their general line apart from the condition on the disc surface which are imposed by the presence of the corona, and some other minor modifications.

### 2.2.2 Equations

We assume the standard viscosity model of Shakura & Sunyaev (1973) with the viscosity proportional to the total (i.e. gas plus radiation) pressure.

We compute the vertical structure using standard equations modified by the presence of convection (Shakura & Sunyaev 1976; Meyer & Meyer-Hofmeister 1981):

$$\frac{1}{\rho} \frac{dP}{dz} = -\Omega_K^2 z, \quad (7)$$

$$P = P_{gas} + P_{rad}, \quad (8)$$

$$F = F_{rad} = -\frac{16\sigma T^3}{3\kappa\rho} \frac{dT}{dz}, \quad \nabla_{rad} \leq \nabla_{ad}, \quad (9)$$

$$F = F_{rad} + F_{conv}, \quad \nabla_{rad} > \nabla_{ad}. \quad (10)$$

We assume that only a fraction of the flux  $F_c$  is generated inside the disc due to the viscous forces and the disc carries away only the same fraction of angular momentum flux (local viscosity model). We therefore follow the main line of reasoning underlying the accreting corona models discussed by Nakamura & Osaki (1993), Życki et al. (1995) and Witt et al. (1997). This assumption is not a unique possibility. Some authors assumed that the disc carries the entire angular momentum flux even if only a fraction of energy is dissipated there (global viscosity model) (e.g. Svensson & Zdziarski 1994, Życki et al. 1995, Sincell & Krolik 1997). We discuss this problem in Section 3.

The influence of hot corona appears through the boundary condition. One of the effects is the illumination of the disc surface by X-ray radiation flux generated in the corona. We assume that half of the flux  $F_c$  is directed toward the disc and all of it is absorbed (albedo equals zero) by the disc matter and than reemitted with addition to the flux dissipated in the main body of the disc:

$$\frac{dF}{dz} = \frac{3}{2}\alpha P\Omega_K + \frac{1}{2}F_c\kappa\rho \exp(-\tau). \quad (11)$$

The opacity  $\kappa$  (the Rosseland mean) as a function of density and temperature is taken from Alexander, Johnson & Rypma (1994) for  $\log T < 3.8$ , from Seaton et al. (1994) for  $\log T > 4.0$  and it is interpolated between these two tables for intermediate values of the temperature.

In the present paper we use the same description for opacity of the incident X-ray photons and of diffusing UV photons. It means an error up to a factor of few since the absorption of hard X-ray photons at  $\sim 100$  keV can be approximately described by opacity  $\sim 0.5$  of the scattering opacity while in soft X-rays the absorption of the photons by a matter of the typical considered ionization stage is of order of 10 times larger than the Thompson cross section. Other authors describing the X-ray heating also use some kind of approximation e.g. Sincell & Krolik (1997). Full treatment of this problem including hydrostatic equilibrium is still to be done and we will address it in the future.

The role of convection is important even if it carries not more than  $\sim 30\%$  of the flux. Here we adopt a simple description of the convection based on mixing length theory used in stellar interiors. This method incorporates the radiation pressure gradient in the optically thick gas but it is not appropriate in the optically thin surface layers (Smak 1982a, Meyer & Meyer-Hofmeister 1981,1982). Actual calculations of the disc structure are done using the code described by Pojmański (1986) and applied to AGN by Siemiginowska, Czerny & Kostyunin (1996); thermodynamic functions are calculated as in Paczyński (1969). The effect of partial ionization of the gas whilst calculating the mean molecular weight,  $\mu$ , is included (whenever necessary).

Equations (7) – (11) are integrated from the top of the disc, assumed to be at  $z = H_d$ , toward the equatorial plane,

with the initial values for  $F$ ,  $T$ , and  $\rho$  given by the boundary conditions at the bottom of the corona.

At the equatorial plane we require:

$$F(z = 0) = 0. \quad (12)$$

This condition actually determines  $H_d$ . We solve this two point boundary problem by a shooting method. The integration is performed by the second order Runge–Kutta scheme with adaptive stepsize. In the absence of the corona ( $f = 0$ ) the required gas pressure at the surface is zero, i.e., consistently, there is no dynamical influence of the corona on the disc structure.

### 2.3 The vertical structure of the corona

In the most general case the influence of the corona on the disc structure is given by the coronal X-ray radiation flux (i.e. the fraction of energy generated in the corona) and the pressure at the bottom of the corona. In order to reduce these two arbitrary parameters to a single arbitrary parameter we make the following assumptions about the corona.

We assume that the corona is in hydrostatic equilibrium so the pressure at the bottom is given by

$$P = \frac{2}{\pi}\rho\Omega_K^2 H_c^2, \quad (13)$$

where  $H_c$  is the scale high of the corona.

We describe the thermal balance in the corona as in the paper of Shapiro, Lightman & Eardley (1976) in the version applied in the coronal paper of Haardt & Maraschi (1991), i.e. the corona is two-temperature, with heating of ions, Coulomb transfer of the energy from ions to electrons and Compton cooling of electrons:

$$P = \frac{k}{m_H}\rho T_i, \quad (14)$$

$$F_c = AF_{soft}; \quad F_{soft} = 0.5F_c + F_d, \quad (15)$$

where  $A$  is the Comptonization amplification factor.

In the present paper the Comptonization amplification factor is computed using our comptonization Monte Carlo code.. The code is based on the method developed by Pozdnyakov, Sobol & Sunyaev (1983). We have implemented this method as described by Górecki & Wilczewski (1984). We have assumed slab geometry and a black body soft photon input and we computed the amplification factor on a grid of  $T_{bb}$ ,  $kT_e$  and optical depth of corona  $\tau_c$ , and then interpolated it to values of interest.

The dependence of our amplification factor on the coronal optical depth is shown on Fig. 1 for different values of  $T_{bb}$  and  $kT_e$ . We compare our values with two analytical approximations for  $A$ . The first approximation (dotted line) was given by Dermer, Liang & Canfield (1991), and second one (dashed line) is  $A = e^y - 1$ , where the Compton parameter in the corona is:  $y = \kappa_{es}\rho H_c(\kappa_{es}\rho H_c + 1)4kT_e/m_e c^2 (1 + 4kT_e/m_e c^2)$ .

All slopes do not depend significantly on the temperature of soft radiation from the disc  $T_{bb}$ . They are similar even for the case of an accretion discs in AGNs ( $T_{bb} \sim 4\text{eV}$ ) and for accretion discs around galactic black holes ( $T_{bb} \sim 100\text{eV}$ ).

The formula of Dermer et al. (1991) differs from our

Monte Carlo values, mainly because our input photon spectrum is a blackbody whilst they considered monoenergetic input. Also, their most important parameter is the effective optical depth which has to be fitted for a given soft photons input energy.

The second analytical approximation is fairly accurate for low electron temperatures and optical depths i.e. when  $y < 1$ . Although for small  $\tau_c$  and high  $T_e$  it becomes inaccurate due to non-diffusive character of Compton scattering in that regime.

The cooling of ions in the corona by the electron-ion Coulomb interaction is described by the following equation (Shapiro, Lightman & Eardley 1976)

$$F_c = \frac{3k(T_i - T_e)}{2m_H} \left[ 1 + \left( \frac{4kT_e}{m_e c^2} \right)^{1/2} \right] \int_{z_0}^{\infty} \nu_{ei} \rho dz, \quad (16)$$

where  $T_i$ ,  $T_e$  are the ion and electron temperatures, and

$$\nu_{ei} = 2.44 \times 10^{21} \rho T_e^{-1.5} \ln \Lambda \quad [(\text{s})^{-1}]; \quad \text{with } \ln \Lambda \approx 20 \quad (17)$$

is the electron-ion coupling rate.

Finally, we assume that the bottom of the corona is defined by achievement of the thermal instability of the irradiated gas and a rapid switch from Compton cooling to atomic cooling, as described by Krolik et al. (1981) and applied to the disc/corona transition by Róžańska (1997). The ionization parameter  $\Xi$

$$\Xi = \frac{F}{cP_{\text{gas}}} \quad (18)$$

is fixed at the bottom of the corona by the scaling properties of its value with the temperature (Begelman, McKee and Shields 1983)

$$\Xi_b = 0.65(T_e/10^8)^{-3/2} \quad (19)$$

The structure of the corona is therefore uniquely described by the coronal flux  $F_c$ , or a fraction  $f$  of the energy liberated in the corona for a given accretion rate. The equations are equivalent to equations used by (Witt, Czerny & Życki 1997) in Appendix D apart from their equation (D4) which requires an additional assumption of viscous energy generation in the corona, not used in the present paper.

## 2.4 The boundary conditions between the disc and the corona

We use the Eddington approximation on the disc surface and we assume for  $\tau = 0$ :

$$F(H_d) = F_{\text{soft}}, \quad (20)$$

$$\sigma T^4(H_d) = \frac{1}{2} \sigma T_{\text{eff}}^4 = \frac{1}{2} F_{\text{soft}} \quad (21)$$

Next boundary condition results from the value of the pressure at the basis of the corona and the requirement of the hydrostatic equilibrium between the disc and the corona

$$\rho_s = \frac{F_c}{2c\Xi} \frac{\mu m_H}{kT}. \quad (22)$$

We take into account only gas pressure since corona generally reduces the radiation pressure.

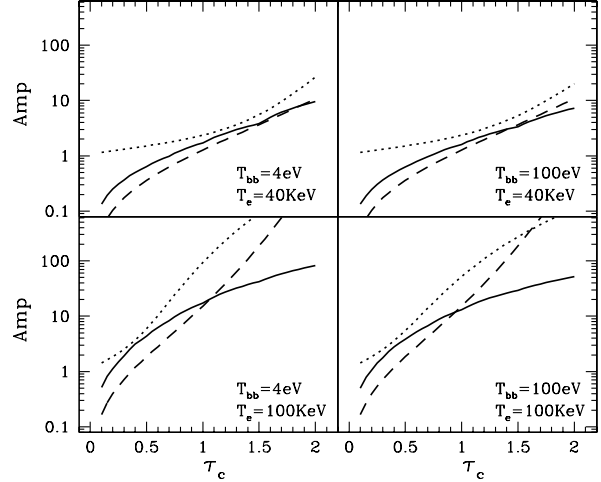


**Figure 1.** Amplification factors for Comptonization versus optical depth of corona computed in three different methods: monte carlo simulations - solid line; approximation by Dermer (1991) - dotted line; analytical approximation  $A = e^y - 1$  - dashed line.  $T_e$  is the temperature of electrons in corona and  $T_{bb}$  is the temperature of soft radiation from the disc. Other parameters are: radius  $r = 10R_{Schw}$ ,  $M = 10^8 M_\odot$ ,  $\dot{m} = 0.03$

## 3 RESULTS

All the numerical results shown are computed at the radius  $10R_{Schw}$  being fairly representative for the innermost part of the disc responsible for generating most of the energy, where  $R_{Schw}$ , the Schwarzschild radius, equals  $2GM/c^2$ . Central black hole mass and viscosity parameter in disc and corona are taken:  $M = 10^8 M_\odot$ ,  $\alpha = 0.1$ .

To show the vertical profiles of the physical quantities we choose an accretion rate (in units of the Eddington accretion rate)  $\dot{m} = 0.03$ , a value fairly representative for Seyfert galaxies.

### 3.1 Corona properties

In this paper we do not concentrate on the properties of the corona itself and the production of hard X-ray emission. This problems are extensively studied by Witt et al.(1997) and Janiuk & Czerny (1998) in the specific context of accreting corona model.

However, in order to illustrate the basic corona properties which might be important from the point of view of the conditions on the disc surface we show the dependence of the coronal optical depth, ion and electron temperature and the pressure scale height in the corona on the assumed fraction of energy generated in the corona  $f$  (see Fig. 2).

We see that the ion temperature is generally not much higher than the electron temperature in our model (Fig. 2 a,b). This is different from other models of corona (Witt et al. 1997) when the equation of energy generated in corona is taken into account. We plan to consider such a corona above an accretion disc in the future.

The optical depth of the corona increases with  $f$ . The corona is optically thin for  $f \lesssim 0.5$  (Fig. 2c). Since the opacity in corona is dominated by electron scattering, the col-

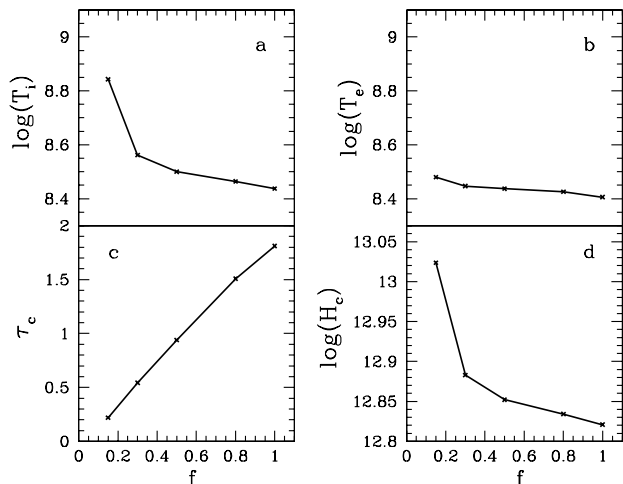


**Figure 2.** Dependence of the coronal a) ion temperature  $T_i$ , b) electron temperature  $T_e$ , c) optical depth  $\tau_c$  and d) pressure scale height  $H_c$  on the fraction of energy generated in the corona. Other parameters are: radius  $r = 10R_{Schw}$ ,  $M = 10^8 M_\odot$ ,  $\dot{m} = 0.03$

umn density in the corona is of order of  $\Sigma_c = \tau_c/\kappa_{es} \sim 1 - 5 \text{ g cm}^{-2}$ .

Fig. 2d shows that under the condition of hydrostatic equilibrium the height of the corona is of order of  $\sim 7 \times 10^{12}$  cm, similar to the disc thickness (see below).

### 3.2 The effect of the corona weight on the disc surface layers

The presence of the corona modifies the conditions close to the surface of the disc. In the absence of the corona the density at the disc surface is zero, consequently the gas close to the surface is fully ionized and the opacity is reduced to electron scattering. However, even energetically weak corona imposes certain pressure at the disc surface so the density at the surface is finite, and it can be quite large (Fig. 5b-f).

Let us first consider an atmosphere in an accretion disc without a corona. The column density  $\Sigma_{ph}$  above the photosphere is of order of  $\Sigma_{ph} = \tau_{ph}/\kappa_{es} \sim 2 \text{ g cm}^{-2}$  since the opacity in the case is dominated by the electron scattering. If such a photosphere has the temperature of order of the effective temperature of the disc  $T_{ph} \sim T_{eff} \sim 4 \times 10^4$  K appropriate for the parameters adopted in the computations ( $M = 10^8 M_\odot$ ,  $r = 10R_{Schw}$ ,  $\alpha = 0.1$ ,  $\dot{m} = 0.03$ ) then the scale height of such a photosphere is of order of

$$H_{ph} = \left( \frac{kT_{ph}}{\mu m_H} r^3 / GM \right)^{1/2} \sim 8 \times 10^{10} \text{ cm} \quad (23)$$

and the pressure imposed by the photosphere is

$$P_{ph} = \frac{GM}{r^3} \Sigma_{ph} H_{ph} \sim 85 \text{ erg cm}^{-3} \quad (24)$$

However, if a hot corona develops it has column density of the same order as the disc photosphere, but since its ion temperature is of order of  $10^9$  K, its scale height is two orders of magnitude higher (Fig. 2 d) and the pressure imposed on the disc surface is higher by the same factor.

This pressure changes the density profile close to the

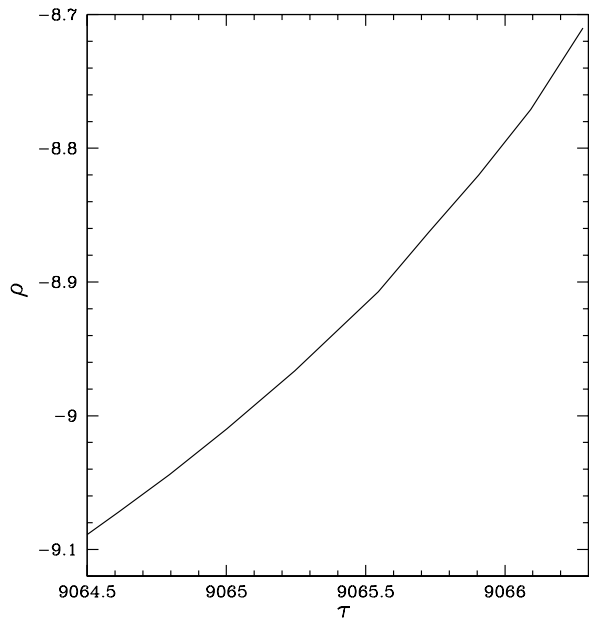


**Figure 3.** Density profile close to the convective disc surface for  $f = 0.5$ .

disc surface leading to more complex behavior than in the disc without the corona.

The density at the disc surface is much higher than in the case of a bare disc. The initial high value of the density decreases towards the disc interior forming the outer layer of the density inversion (for inner one – see Sec. 3.3). The effect is caused by the dynamical pressure of the corona. We can see the role of the surface pressure from an approximate expression

$$\frac{d\rho}{d\tau} = \frac{2}{3} \frac{g}{\kappa_0} - \frac{1}{4} P_0 - \frac{1}{8} a T_{eff}^4 < 0 \quad (25)$$

where  $P_0$  and  $\kappa_0$  are the pressure and opacity coefficient at the disc surface, and  $g$  is the surface gravity given by  $GMH_d/r^3$ . The region of density inversion is dynamically unstable which results in the development of convection (Hansen & Kawaler 1994). Convection, however, is actually very inefficient in this zone according to our present computations, in opposite to convection which develops in the disc interior (see Section 3.3). It remains to be seen whether this conclusion would change after introducing better description of the radiative transfer in the disc surface layers since it may change significantly the temperature gradient close to the disc surface.

The increased value of the density close to the surface leads to a layer of increased opacity (Fig. 7). Therefore, whilst for a disc model without a corona the opacity at  $\tau = 2/3$  is dominated by the electron scattering, for a disc with a corona (e.g. for  $f = 0.3$ ) the opacity there is clearly dominated by bound-free opacities. What is more, the density at  $\tau = 2/3$  is also significantly different in those two cases: it is equal  $8.8 \times 10^{-11} \text{ g cm}^{-3}$  for a bare disc and  $1.24 \times 10^{-9} \text{ g cm}^{-3}$  for the model with  $f = 0.5$ . The expanded plot of the density and opacity profiles close to the disc surface is shown in Fig. 3 and Fig. 4.

Therefore, the density in the region where the disc spectrum forms is not much lower than the density at the equa-

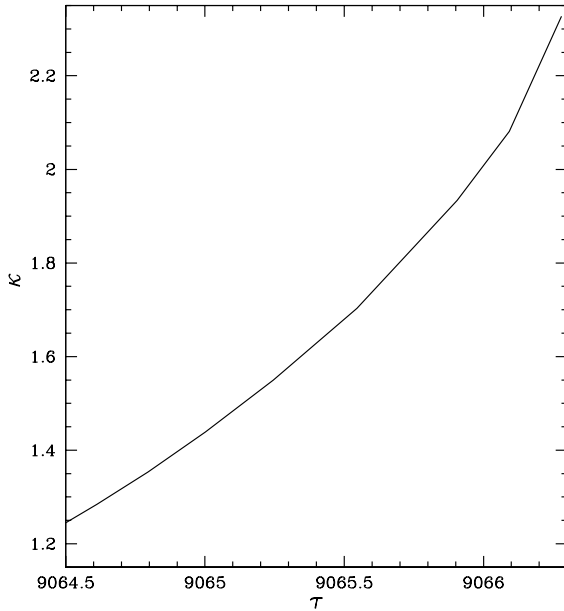


**Figure 4.** Opacity profile close to the convective disc surface for  $f = 0.5$ .

torial plane – or even higher for strong coronae. It is more than an order of magnitude lower than the mean density calculated from the formula of Shakura & Sunyaev (1973)

$$n^{SS} = 8.3 \times 10^{16} \alpha^{-1} \dot{m}^{-2} m^{-1} x^{3/2} f(x)^{-2} \quad (26)$$

where  $x = r/R_{Schw}$  and  $m = M/10^8 M_\odot$  which gives the value  $n = 2 \times 10^{15} \text{ cm}^{-2}$  (or  $\rho = 3.35 \times 10^{-9} \text{ g cm}^{-3}$ ) for the model shown in Fig. 3.

The density at the disc surface,  $\rho_s$ , depends only weakly on accretion rate as it is shown in Fig. 9 for  $f = 0.3$  and  $f = 0.8$ . Since the effective temperature increases with increasing  $\dot{m}$ , the density at  $\tau = 2/3$  decreases with increasing  $\dot{m}$ .

### 3.3 The effect of the corona on the disc interior

The results presented in this section depend significantly on the assumption that the disc carries only the fraction of the angular momentum proportional to the fraction of the energy generated there. Therefore, if e.g. almost all energy is released in the corona ( $f \approx 1$ ) the disc becomes almost isothermal (since it is only heated from outside by the incident X-ray flux), geometrically very thin and dense. Its surface density  $\Sigma$  is slightly lower than in the case of a disc without a corona.

The profiles of temperature and density in the vertical direction are very flat throughout most of the disc interior (Fig. 5 and Fig. 6). Their values change rapidly only near the surface.

A noticeable feature is the density inversion at the optical depth of the order of 100 (inner density inversion) which occur irrespectively of the presence or absence of the corona until the corona becomes very strong. The possibility of this inversion can be seen from the density gradient expression,

$$\frac{d\rho}{dz} = \left[ \frac{dP}{dz} - \left( \frac{\partial P}{\partial T} \right)_\rho \frac{dT}{dz} \right] / \left( \frac{\partial P}{\partial \rho} \right)_T, \quad (27)$$

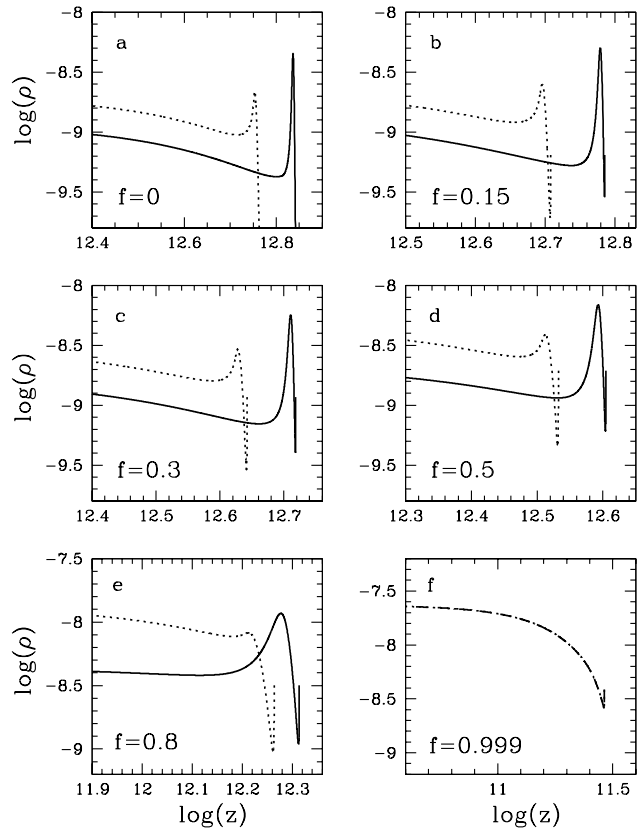


**Figure 5.** The density profiles in the accretion disc with convection (dotted line) and without convection (solid line) for a)  $f = 0$  - bare disc; b)  $f = 0.1$  - disc with weak corona; c)  $f = 0.3$ , d)  $f = 0.5$  - disc with moderate corona; e)  $f = 0.8$  disc with strong corona. In the case when almost all energy is dissipated in corona - f)  $f = 0.999$ , it is no difference between disc with convection (dotted line) and without convection (short dashed line). Other parameters are: radius  $r = 10R_{Schw}$ ,  $M = 10^8 M_\odot$ ,  $\dot{m} = 0.03$

which allows for inversion if the temperature gradient is large enough.

Such a density inversion is well known in some classes of stars, like supergiants (see e.g. Heger & Langer 1998 for a recent study of supergiant envelopes). This region is dynamically unstable which results in the development of convection (Hansen & Kawaler 1994) which has to be included in the computation of the stellar structure throughout this region although heat transport by convection is not always efficient. The effect is usually caused either by distribution of energy sources or by opacity in partial ionization zone.

Similar situation takes place in the accretion disc interior. Radiation pressure dominates throughout the bare disc ( $\beta \equiv P_{\text{gas}}/(P_{\text{gas}} + P_{\text{rad}}) \lesssim 0.01$ ) for  $\dot{m} \gtrsim 0.03$ . The energy flux to be transported rises approximately linearly with the distance from the equatorial plane, therefore, further out from the equatorial plane, where pure radiative transfer would cause difficulties, a fraction of the energy is carried out by convection. This is demonstrated in Fig. 5 where we plot density profiles in the case with and without convection for different fractions of energy dissipated in corona  $f$ . Fig. 5a-e show that convection dominates in the disc interior

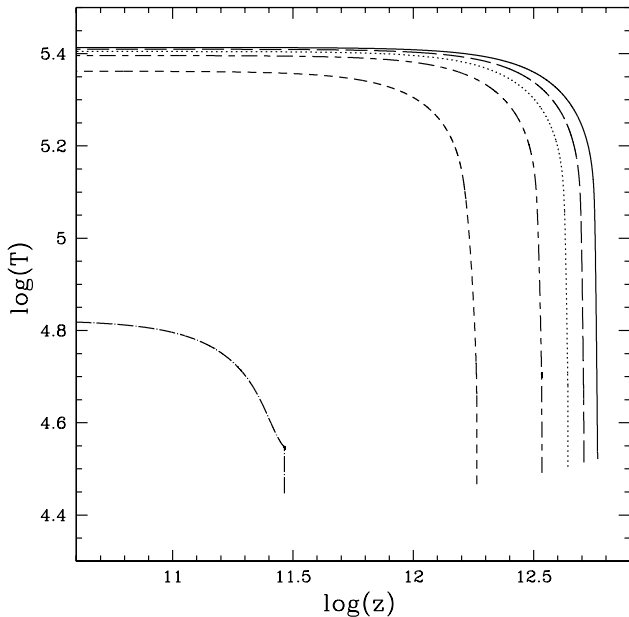


**Figure 6.** The temperature profile in the convective accretion disc without corona ( $f = 0$ ; continuous line), with weak corona ( $f = 0.1$ ; long dashed line) with moderate corona ( $f = 0.3$ ; dotted line), ( $f = 0.5$ ; short dashed long dashed line), with strong corona ( $f = 0.8$ ; short dashed line), with corona which dissipates all energy ( $f = 1$ ; dashed dotted line). Other parameters are: radius  $r = 10R_{Schw}$ ,  $M = 10^8 M_{\odot}$ ,  $\dot{m} = 0.03$

and, modifying the density profile, reduces the inner density inversion. These results are in agreement with calculations done by Milson et al. (1994) for accretion disc around low mass black holes and neutron stars. For the black hole of  $10M_{\odot}$  convection smoothes out inversion almost completely (Milson et al. 1994 Fig. 2b). Comparing the gradients: adiabatic, radiative and the gradient  $\nabla = d \log T / d \log \rho$  actually achieved in the disc interior we calculated that the convection carries significant fraction of the flux ( $\sim 30\%$ ).

Another phenomenon which reduces inner density inversion is the presence of a corona. Note that for bare disc the inversion is strongest. Stronger corona leads to lower inversion and for  $f = 0.999$  this effect disappears completely. When almost all energy is dissipated in the corona (Fig. 5f) the disc is squeezed to the thin and dense slab with purely radiative energy transport.

### 3.4 The comparison with global viscosity model

The results are quite different if the disc has to carry the total angular momentum flux. In such case strong viscous stress has to operate within the cold disc even if the energy is generated entirely in the corona. Numerically, such computations correspond to the change of the surface boundary condition for equation (11) from  $F_d + F_X$  (where  $F_X$  is the incident X-ray flux) to  $F_d + F_c + F_X$ .

The pressure in the disc interior has now to be high in order to provide the integrated stress high enough to transport the angular momentum, even if the disc does not dissipate the energy. Therefore the disc column density for e.g.  $f = 0.999$  is much higher than under the assumptions adopted previously.

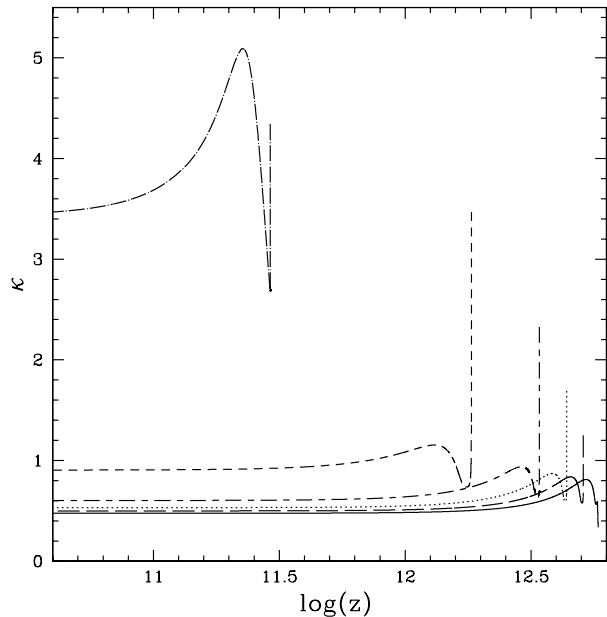


**Figure 7.** The profile of the opacity in the convective accretion disc without corona ( $f = 0.1$ ; long dashed line), with weak corona ( $f = 0.1$ ; long dashed line) with moderate corona ( $f = 0.3$ ; dotted line), ( $f = 0.5$ ; short dashed long dashed line), with strong corona ( $f = 0.8$ ; short dashed line), with corona which dissipates all energy ( $f = 1$ ; dashed dotted line). Other parameters are: radius  $r = 10R_{Schw}$ ,  $M = 10^8 M_{\odot}$ ,  $\dot{m} = 0.03$

We show examples of solutions for the density profiles in Fig. 8 for different values of  $f$  (the same as in Fig. 5 for local viscosity model). We see that for  $f$  close to 1 the density in the disc interior is much higher than in the local viscosity model, keeping the same structure near the surface.

For global viscosity model, in case where almost all energy is dissipated in corona ( $f = 0.999$ ) the column density of the disc is higher of the order of two magnitude than in our previous approach (Fig.5 f and Fig.8 f). This is not surprising since global viscosity model requires the disc to transport the entire angular momentum while in case of corona transporting the angular momentum as well as dissipating the energy, the role of the disc is reduced to reprocessing half of the X-ray emission.

## 4 LYMAN EDGE AND IONIZATION STATE OF THE DISC MATTER

In this paper we do not calculate the spectrum of the disc with the corona since further developments of the model are necessary before we can do that reliably (see Discussion). However we have shown above that the corona modifies the layer where spectrum is formed, making this layer denser and dominated by bound-free absorption. In this situation the electron scattering is not important any more and we can expect not to see Lyman edge in emission. Such an emission edge is predicted in all models computed for bare but irradiated discs (Sincell & Krolik 1997), but it does not appear in any observed spectrum.

Simple estimates of the dependence of Lyman edge magnitude on effective temperature and density of emit-

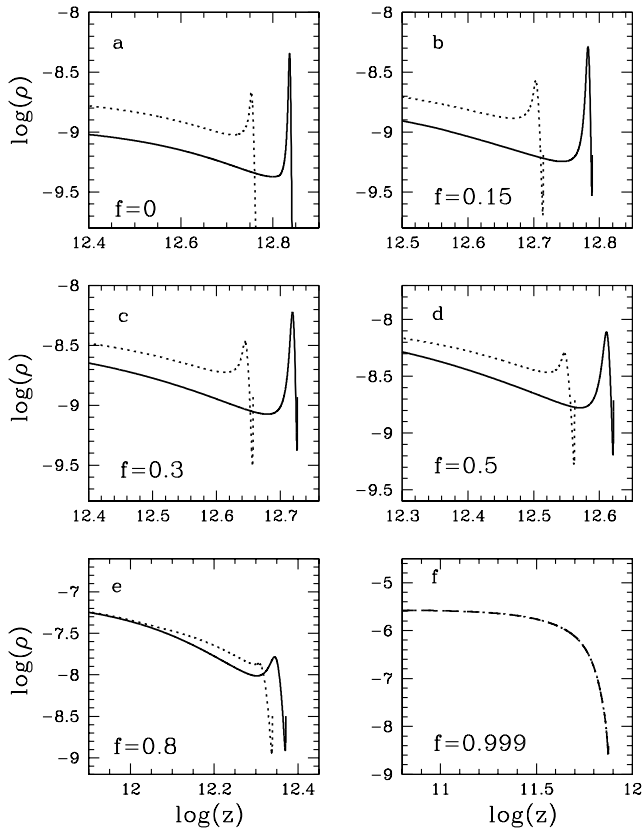


**Figure 8.** The density profiles for global viscosity model of the accretion disc with convection (dotted line) and without convection (solid line) for a)  $f = 0$  - bare disc; b)  $f = 0.1$  - disc with weak corona; c)  $f = 0.3$ , d)  $f = 0.5$  - disc with moderate corona; e)  $f = 0.8$  disc with strong corona. In the case when almost all energy is dissipated in corona - f)  $f = 0.999$ , it is no difference between disc with convection (dotted line) and without convection (short dashed line). Other parameters are: radius  $r = 10R_{Schw}$ ,  $M = 10^8 M_\odot$ ,  $\dot{m} = 0.03$

ting layer were done by Czerny & Pojmański (1990). They shown the reduction of Lyman edge for densities higher than  $10^{-7} \text{gcm}^{-3}$  and for wide range of effective temperatures higher than  $5 \times 10^4 \text{K}$ . Trying to apply this prediction to the accretion disc model they concluded that for bare disc the Lyman edge size close to zero corresponds to a very narrow range of accretion rates.

In the our case of accretion discs with hot coronae we assumed Eddington approximation as in Czerny & Pojmański (1990). Making additional assumptions that the expected spectrum is a modified blackbody and the disc inclination angle is  $i = 0^\circ$  we used the same code to calculate the Lyman edge for various densities and effective temperatures resulting from our model.

The computations for several values of accretion rate  $\dot{m} = 0.02 - 0.09$  and  $f$  are presented in Table 1. We can see that for bare discs a strong edge in emission is obtained for all  $\dot{m}$  but for each  $\dot{m}$  there is range of  $f$  such that the edge is very weak.

For  $\dot{m} < 0.02$  the edge is in absorption, independently of the strength of the corona. Larger values of accretion rate al-

**Table 1.** The size of Lyman edge in magnitudes  $\Delta m$  for various  $f$  and  $\dot{m}$ .  $\Delta m < 0$  indicates the edge in emission.

$f$	$\dot{m} = 0.02$	$\dot{m} = 0.03$	$\dot{m} = 0.06$	$\dot{m} = 0.09$
0	-0.7	-0.9	-1.07	-1.13
0.15	-0.14	-0.37	-0.63	-0.76
0.3	-0.01	-0.21	-0.43	-0.56
0.5	0.26	0.02	-0.26	-0.40
0.8	0.58	0.36	-0.07	-0.16
0.999	0.74	0.56	0.14	—

low for an edge both in absorption and in emission, depending on the strength of the corona. For increasing accretion rates the range of  $f$  for which the edge is weak moves towards strong coronae. When the corona is relatively strong, the surface density  $\rho_s$  is high and an edge in absorption is expected if  $\dot{m} \lesssim 0.06$ . Larger accretion rates are characterised by an edge in emission. However, for very high accretion rate ( $\dot{m} = 0.09$ ) strong corona cannot exist in hydrostatic equilibrium and we cannot obtain solutions determining the disc/corona structure.

The presence of corona leads to a wide range of accretion rates for which the Lyman edge is significantly reduced in the spectrum.

Trying to predict some spectral features of our model, we can compare the estimate of the ionization parameter  $\xi$  at the disc/corona surface with the limits derived from the properties of the reflection component. This parameter is usually defined as

$$\xi = \frac{4\pi F}{n} \quad (28)$$

where  $F$  is the incident flux (equal  $0.5F_c$  in our model) and  $n$  is the number density of the irradiated layer (note the essential difference from ionization parameter  $\Xi$  used in equation 19). For the case shown in Fig. 3 ( $f = 0.5$ ) the value of this parameter at the optical depth  $\tau = 2/3$  is equal 0.3 whilst for a disc with the same parameters but without corona, this value is equal 100.

The properties of the interior change dramatically only if almost all the energy is liberated in the corona ( $f > 0.999$ ) and the disc only reprocesses the X-ray radiation. In that case the disc becomes almost isothermal and dominated by the gas pressure. The mean density of the interior is not monotonic as a function of  $\xi$ : the largest density is obtained for intermediate  $\xi$ . This is connected with  $P_{gas}/P_{rad}$  ratio, the maximum  $\rho$  being obtained when both pressures are comparable.

## 5 DISCUSSION

Previous computations of the disc spectra were done by a number of authors (e.g. Shimura & Takahara 1993, Ross, Fabian & Mineshige 1993) but none of these papers treated carefully the disc surface where the radiation spectrum forms so these spectra models are not ready yet for detailed comparison with the observational data.

In this paper we describe the vertical structure of the



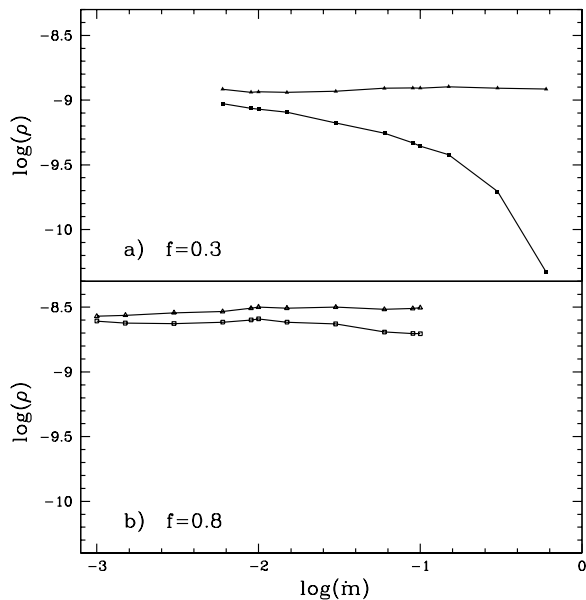


**Figure 9.** The dependence of surface density (triangles), and the density of the layer on  $\tau = 2/3$  (squares), on accretion rate for two cases of corona a)  $f = 0.3$  and b)  $f = 0.8$ . Other parameters are: radius  $r = 10R_{Schw}$ ,  $M = 10^8 M_{\odot}$ .

disc instead of solving algebraic equations for the vertically averaged quantities. It allows us to incorporate properly the effect of the corona, which modifies significantly the outer layers of the disc. A hot corona exerts a dynamically pressure on the disc and changes its surface zone making it denser and dominated by bound – free absorption. The first consequence of the coronal influence is the low ionization state of the matter on the disc surface. This agrees with observations for which we know that X-ray radiation produced in corona reflects from the relatively neutral gas  $\xi \sim \text{few}$  (Pounds et al.1990, Nandra et al. 1994).

The size of Lyman edge close to zero for wide range of accretion rates is the second important consequence of our model. In the observed quasar spectra we do not see Lyman edge, but all bare discs models predict such a feature. Also, recent calculations by Sincell & Krolik (1997) of X-ray heated disc, indicate the presence of emission Lyman edge in the disc spectrum. They considered a layer resulting from X-ray illumination positioned on top of a cold disc. Illumination of plasma by relatively hard X-rays leads to existence of multi-phase medium due to thermal instability (Krolik et al. 1981). If such a situation takes place in accretion discs, then, as shown by Rózańska (1998), the plasma in the transition layer between cold disc and X-ray source forms a two-phase medium. Sincell & Krolik (1997) considered only one, cold phase of the transition layer. Stopping computations just before the temperature runaway they obtained the density of the layer which is one order of magnitude lower than density at the disc surface in our model. Also, the temperature they compute is higher, so they could expect Lyman edge in emission. However, this treatment can overestimate Lyman edge in emission since it does not take into account that transition layer is a mixture of cold and hot phase. In the present approach we also neglected the presence of the

two-phase medium but we replaced the transition zone by a hot, instead of a cold phase which is more appropriate but may lead to some underestimate of the edge in emission.

However, a number of further improvements to the model are necessary before we can reliably calculate the spectrum emitted by such a disc/corona model.

First of all, more careful description of the disc/corona transition is necessary. A fraction of that zone consists of two-phase medium, possibly undergoing continuous, quasi-stationary evolution (Rózańska 1998). Future models should incorporate this transition zone as its optical depth and the temperature profile may have an important effect on the emergent radiation flux.

Further work is needed to improve the description of the X-ray heated upper layers of the disc. Rózańska (1998) showed how important it is in the transition zone. However, her method to iterate between the vertical structure code and Monte Carlo computations of X-ray transfer cannot be repeated directly in the present work since those computations were based on radiative heating and cooling appropriate only for optically thin zone. In order to describe the disc we need a code which solves the radiative transfer in optically thick irradiated medium. Such a code was developed by Collin-Souffrin & Dumont (see Collin-Souffrin et al. 1996, Czerny & Dumont 1998), and we intend to combine it with our description of the disc structure.

A number of improvements can be done for the disc interior as well, although they may not be essential from the point of view of the emitted spectra.

The accretion pattern is more complex than usually considered. Two-dimensional studies of models based on local viscosity  $\alpha$  (Urpin 1984, Siemiginowska 1988, Kley & Lin 1992, Różyńska, Bodenheimer & Bell 1994) showed that for low viscosity there is actually an outflow near equatorial plane and inflow close to the surface; pure inflow is only for high viscosity ( $\alpha > 0.1$ ).

The convection here is described using the standard mixing length theory (with the phenomenological coefficient, also named  $\alpha$ , equal 1). More advanced approach may require correct adjustment of this value (see Cannizzo 1992 for discussion of the convection in the outer, gas dominated, parts of the disc).

We note an advantage of solving the vertical structure of the disc. Frequently, the use of vertically averaged algebraic equations for disc structure leads to unphysical multiple solutions if complex description of opacities is adopted as well as a contribution to the pressure both from gas and radiation is allowed (Cannizzo & Reiff 1992; Huré et al. 1994ab); these multiple solutions vanish if vertical structure of the disc is integrated step by step and, for a given  $\dot{m}$ ,  $r$  and  $\alpha$ , the structure is unique. The uniqueness of solutions is preserved in the case of a disc with a corona.

Finally, as suggested by the stability analysis of the radiation dominated disc and clearly seen in observations, the disc undergoes continuous evolution and the assumption of stationarity can be satisfied only in the sense of time averaged quantities, at best. Recent computations of disc evolution for the case of galactic black holes (Szuszkiewicz & Miller 1998) give the timescales  $\sim 780s$  coinciding nicely with the peak in the power density spectra of these objects (see van der Klis 1995). In the case of AGN only the slow evolution of the outermost, gas dominated, parts of the discs

was properly addressed (see e.g. Siemiginowska, Czerny & Kostyunin 1996 and the references therein).

## 6 CONCLUSIONS

In this paper we show that the presence of the corona changes essentially the physical conditions close to the disc surface. The disc is much denser there and less ionized than a bare disc due to the dynamical pressure of the hot medium. Although at present we do not show yet the radiation spectrum of such a model we expect that the enhanced surface density makes this disc model promising. The reflection from such a disc will not show any signs of high ionization. Also the Lyman edge will be significantly reduced in such a model as the spectrum emitted locally approaches a black body for increasing density. It will remove the basic argument against an existence of an accretion disc in AGN based on the absence of the Lyman edge in the data. Therefore the corona is not only essential from the point of view of X-ray spectra formation but helps to remove the problems with discy models for AGN.

## ACKNOWLEDGEMENTS

We thank J. Smak, Z. Loska and W. Dziembowski for helpful discussions, and the anonymous referee for remarks leading to significant improvement of the paper and clarification of the presented results. This work was supported in part by grant no. 2P03D00410 of the Polish State Committee for Scientific Research.

## REFERENCES

- Alexander D.R., Johnson H.R., Rypma R.L., 1983, *ApJ*, 272, 773  
 Antonucci, R., 1993, *Ann. Rev. A&A*, 31, 473  
 Balbus S.A., Hawley J.H., 1991, *ApJ*, 376, 214  
 Balbus S.A., Hawley J.H., 1992, *ApJ*, 400, 595  
 Balbus S.A., Hawley J.H., 1998, *Rev. of Modern Physics*, 70, 1  
 Begelman M.C., McKee C.F., Shields G.A., 1983, *ApJ*, 271, 70  
 Blaes O., Agol E., 1996, *ApJ*, 469, L41  
 Cannizzo J.K., 1992, *ApJ*, 385, 94  
 Cannizzo J.K., Reiff C.M., 1992, *ApJ*, 385, 87  
 Cannizzo J.K., 1994, in *Accretion Discs in Compact Stellar Systems*, ed. J.C. Wheeler, Singapore: World Scientific  
 Czerny, B., Dumont, A.-M., 1998, *A&A*, 338, 386  
 Canuto V.M., Goldman I., Hubickyj O., 1984, *ApJ*, 280, L55  
 Collin-Souffrin S., Czerny B., Dumont, A.M., Życki P.T., *A&A* 1996, 314, 303  
 Dermer C.D., Liang E.P., Canfield E., 1991, *ApJ*, 369, 410  
 Dörrer T., Riffert H., Staubert R., Ruder, H., 1996, *A&A*, 311, 69  
 Edelson R. et al. 1997, *ApJ* 470, 364  
 Frank J., King A.R., Raine D.J., 1992, *Accretion Power in Astrophysics 2. ed.*, Cambridge Univ. Press, Cambridge  
 Gammie C.F., 1998, *MNRAS*, 297, 929  
 Górecki A, Wilczewski W. 1984, *Acta Astron.*, 34, 141  
 Haardt F., Maraschi L., 1991, *ApJ*, 380, L51  
 Hansen, C.J., Kawaler, S.D., 1994, *Stellar Interiors: Physical Principles, Structure, and Evolution*, Springer-Verlag, New York  
 Hawley S.A., Gammie C.F., Balbus J.F., 1995, *MNRAS*, 271, 197  
 Heger, A., Langer, N., 1998, *A&A*, 334, 210  
 Huré J.-M., Collin-Souffrin S., Le Bourlot J., Pineau Des Fortes G., 1994a, *A&A*, 290, 19  
 Huré J.-M., Collin-Souffrin S., Le Bourlot J., Pineau Des Fortes G., 1994a, *A&A*, 290, 34  
 Janiuk A., Czerny, B., 1998 (submitted)  
 Kley W., Lin D.N.C., 1992, *ApJ*, 397, 600  
 Krolik J.H., McKee C.F., Tarter C.B., 1981, *ApJ*, 249, 422  
 Krolik J.H., 1998, *ApJ*, 498, L13  
 Lin D.N.C., Shields G.A., 1986, *ApJ*, 305, 28  
 Loska Z. Czerny B. 1997, *MNRAS*, 284, 946  
 Meyer F., Meyer-Hofmeister, E., 1981, *A&A*, 104, L10  
 Meyer F., Meyer-Hofmeister, E., 1982, *A&A*, 106, 34  
 Milson J.A., Chen X., Taam R.E., 1994, *ApJ*, 421, 668  
 Mineshige S., Shields G.A., 1990, *ApJ*, 351, 47  
 Mushotzky R.F., Done C., Pounds K.A., 1993, *ARAA*, 31, 717  
 Mushotzky, R.F., Fabian, A.C., Iwasawa, K., Kunieda, H., Mat-suoka, M., Nandra, K., Tanaka, Y., 1995, *MNRAS*, 272, L9  
 Nakamura, K., Osaki, Y., 1993, *PASJ*, 45, 775  
 Nandra K., Pounds K.A. 1994, *MNRAS*, 268, 405  
 Nandra K., Mushotzky R.F., Yaqoob T., George I.M., Turner T.J., 1997b, *MNRAS*, 284, L7  
 Narayan, R., Kato, S., Honma, F., 1997, *ApJ*, 476, 49  
 Paczyński B., 1969, *Acta Astron.*, 19, 1  
 Pojmański G., 1986, *Acta Astron.*, 36, 69  
 Pounds K.A., Nandra K., Stewart G.C., George I.M., Fabian A.C., 1990, *Nature*, 344, 132  
 Pozdnyakov L. A., Sobol I. M., Sunyaev R. A. 1983, *Ap. Space Phys. Rev.*, 2, 189  
 Pringle J.E., Rees M.J., Pacholczyk A.G., 1973, *A&A*, 29, 179  
 Ross R.R., Fabian A.C., Mineshige S., 1992, *MNRAS*, 258, 189  
 Ross R.R., Fabian A.C., 1993, *MNRAS*, 261, 74  
 Różańska A. 1998, *MNRAS* (submitted and reviewed).  
 Różyczka M., Bodenheimer P., Bell K.R., 1994, *ApJ*, 423, 736  
 Seaton M.J., Yan Y., Mihalas D., Pradhan A.K., 1994, *MNRAS*, 266, 805  
 Shakura N.I., Sunyaev R.A. 1973, *A&A*, 24, 337  
 Shakura N.I., Sunyaev R.A. 1976, *MNRAS*, 175, 613  
 Shapiro S.L., Lightman A.P., Eardley D.M., 1976, *ApJ*, 204, 187  
 Shimura T., Takahara F., 1993, *ApJ*, 419, 78  
 Siemiginowska A., 1988, *Acta Astron.*, 38, 21  
 Siemiginowska A., Czerny B., Kostyunin V., 1996, *ApJ*, 458, 491  
 Sincell M.W., Krolik J.H., 1997 *ApJ*, 476,605  
 Smak J.I., 1982a, *Acta Astron.*, 25, 227  
 Smak J.I., 1982b, *Acta Astron.*, 32, 199  
 Svensson, R., Zdziarski, A.A., 1994, *ApJ*, 436, 599  
 Szuszkiewicz, E., Miller, J.C., 1998, *MNRAS*, 298, 888  
 Tanaka, Y., et al., 1995, *Nat.*, 375, 659  
 Tout C.A., Pringle J.E., 1992, *MNRAS*, 259, 604  
 Urpin V.A., 1984, *Sov. Astron.*, 28, 50  
 Van der Klis, M., 1995, in *X-ray Binaries*, eds. W.H.G. Lewin, J. van Paradijs & E.P.J. van den Heuvel, Cambridge University Press, p. 252  
 Yaqoob, T., Serlemitsos, P.J., Turner, T.J., George, I.M., Nandra, K., 1996, *ApJ*, 470, L27  
 Witt H.J., Czerny B., Życki P.T., 1997, *MNRAS*, 286, 848  
 Życki, P.T., Collin-Souffrin, S., Czerny, B., 1995, *MNRAS* 277, 70  
 Życki P.T., Krolik J.H., Zdziarski A.A., Kalman T.R., 1994, *ApJ*, 437, 597

This paper has been processed by the authors using the Blackwell Scientific Publications L<sup>A</sup>T<sub>E</sub>X style file.